

# Knowledge transfer of Deep Learning for galaxy morphology from one survey to another

H. Domínguez Sánchez<sup>1\*</sup>, M. Huertas-Company<sup>1,2,3</sup>, M. Bernardi<sup>1</sup>, S. Kaviraj<sup>4</sup>, J.L. Fischer<sup>1</sup>, T. M. C. Abbott<sup>5</sup>, F. B. Abdalla<sup>6,7</sup>, J. Annis<sup>8</sup>, S. Avila<sup>9</sup>, D. Brooks<sup>6</sup>, E. Buckley-Geer<sup>8</sup>, A. Carnero Rosell<sup>10,11</sup>, M. Carrasco Kind<sup>12,13</sup>, J. Carretero<sup>14</sup>, C. E. Cunha<sup>15</sup>, C. B. D’Andrea<sup>1</sup>, L. N. da Costa<sup>10,11</sup>, C. Davis<sup>15</sup>, J. De Vicente<sup>16</sup>, P. Doel<sup>6</sup>, A. E. Evrard<sup>17,18</sup>, P. Fosalba<sup>19,20</sup>, J. Frieman<sup>8,21</sup>, J. García-Bellido<sup>22</sup>, E. Gaztanaga<sup>19,20</sup>, D. W. Gerdes<sup>17,18</sup>, D. Gruen<sup>15,23</sup>, R. A. Gruendl<sup>12,13</sup>, J. Gschwend<sup>10,11</sup>, G. Gutierrez<sup>8</sup>, W. G. Hartley<sup>6,24</sup>, D. L. Hollowood<sup>25</sup>, K. Honscheid<sup>26,27</sup>, B. Hoyle<sup>28,29</sup>, D. J. James<sup>30</sup>, K. Kuehn<sup>31</sup>, N. Kuropatkin<sup>8</sup>, O. Lahav<sup>6</sup>, M. A. G. Maia<sup>10,11</sup>, M. March<sup>1</sup>, P. Melchior<sup>32</sup>, F. Menanteau<sup>12,13</sup>, R. Miquel<sup>14,33</sup>, B. Nord<sup>8</sup>, A. A. Plazas<sup>34</sup>, E. Sanchez<sup>16</sup>, V. Scarpine<sup>8</sup>, R. Schindler<sup>23</sup>, M. Schubnell<sup>18</sup>, M. Smith<sup>35</sup>, R. C. Smith<sup>5</sup>, M. Soares-Santos<sup>36</sup>, F. Sobreira<sup>37,10</sup>, E. Suchyta<sup>39</sup>, M. E. C. Swanson<sup>13</sup>, G. Tarle<sup>18</sup>, D. Thomas<sup>9</sup>, A. R. Walker<sup>5</sup>, and J. Zuntz<sup>40</sup>

17 July 2022

*Author affiliations are listed at the end of this paper*

## ABSTRACT

Deep Learning (DL) algorithms for morphological classification of galaxies have proven very successful, mimicking (or even improving) visual classifications. However, these algorithms rely on large training samples of labeled galaxies (typically thousands of them). A key question for using DL classifications in future Big Data surveys is how much of the knowledge acquired from an existing survey can be exported to a new dataset, i.e. if the features learned by the machines are meaningful for different data. We test the performance of DL models, trained with Sloan Digital Sky Survey (SDSS) data, on Dark Energy survey (DES) using images for a sample of 5000 galaxies with a similar redshift distribution to SDSS. Applying the models directly to DES data provides a reasonable global accuracy ( $\sim 90\%$ ), but small completeness and purity values. A fast domain adaptation step, consisting in a further training with a small DES sample of galaxies ( $\sim 500$ -300), is enough for obtaining an accuracy  $> 95\%$  and a significant improvement in the completeness and purity values. This demonstrates that, once trained with a particular dataset, machines can quickly adapt to new instrument characteristics (e.g., PSF, seeing, depth), reducing by almost one order of magnitude the necessary training sample for morphological classification. Redshift evolution effects or significant depth differences are not taken into account in this study.

**Key words:** galaxies: structure – methods: observational – surveys

## 1 INTRODUCTION

Astronomy is entering the Big Data era. We are experiencing a revolution in terms of available data thanks to surveys such as COSMOS (Scoville et al. 2007), SDSS (Eisenstein et al. 2011), DEEP2 (Newman et al. 2013), DES (DES Collaboration et al. 2016), etc. The close future is even brighter with missions like EUCLID (Racca et al. 2016) or LSST

(LSST Science Collaboration et al. 2017), offering photometric, quasi-spectroscopic data of millions/billions of galaxies.

One key measurement severely affected by this Big Data transition is galaxy morphology estimated from images. Galaxies exhibit a great variety of shapes and their morphology is closely related to their stellar content. In addition, the light-profiles provide information about their mass-assembly, interactions, accretion, quenching processes or feedback (e.g. Conselice 2003; Kaviraj 2014; Bournaud et al. 2014; Belfiore et al. 2015; Dubois et al. 2016). It is

\* Corresponding author: helenado@sas.upenn.edu

therefore crucial to have accurate morphological classifications for large samples of galaxies.

Galaxy morphological catalogues have been usually based on visual classifications. Unfortunately, visual classification is an incredible time consuming task. The size of present and future Big Data surveys, containing millions of galaxies, make this approach a near impossible task. One beautiful solution to this problem was the Galaxy Zoo project (Lintott et al. 2011), which involved more than 100,000 volunteer citizens to morphologically classify the full SDSS sample and has now been extended to other higher redshifts and surveys (e.g. CANDELS survey, Simmons et al. 2016; DECaLS survey). However, with the next generation of surveys, we are reaching the limit of applicability of these approaches. It is estimated that about a hundred years would be needed to classify all data from the EUCLID mission with a Galaxy Zoo-like approach, unless the number of people involved is significantly increased. A question naturally arises: can human classifiers be replaced by algorithms?

Automated classifications using a set of parameters that correlate with morphologies, e.g. CAS-methods (Concentration-Asymmetry-Smoothness, Conselice 2003) or Principal Component Analysis (Lahav et al. 1995, 1996; Banerji et al. 2010, and references therein) have been attempted. However, the parameter extraction also requires large amounts of time. DL algorithms where, in contrast to classic machine learning algorithms, no image pre-processing is needed, have come to the rescue for image analysis of large data surveys. The use of convolutional neural networks (CNNs) to learn and extract the most meaningful features at pixel level have been shown to produce excellent results for pattern recognition in complex problems and are widely used by many technology giants such as *Google*. CNNs have demonstrated their success for morphological classification of galaxies in The Galaxy Challenge<sup>1</sup>, a Kaggle competition for reproducing the Galaxy Zoo 2, where the top three algorithms used CNNs (e.g. Dieleman et al. 2015). At higher redshifts, Huertas-Company et al. 2015 also showed that CNNs represent a major improvement with respect to CAS-based methods.

In a companion paper, Domínguez Sánchez et al. (2018, DS18 hereafter), we combine the best existing visual classification catalogues with DL algorithms to provide the largest (670,000 galaxies from DR7-SDSS survey) and most accurate morphological catalogue to date. The catalogue includes two flavours: T-Type, related to the Hubble sequence, and Galaxy Zoo 2 classification scheme. One of the main improvements with respect to previous works (Dieleman et al. 2015), is that only galaxies with robust classifications (large agreement between Galaxy Zoo classifiers) are used for training each task. This helps the models to detect the relevant features for each question and a smaller training sample is required for the models to converge.

In spite of this improvement on the training approach, these algorithms still rely on large training sets (around 5000-10000 galaxies, depending on the classification task). A key question, in view of using DL based algorithms to assess the morphologies of galaxies in future Big Data surveys, is therefore how much of the knowledge acquired from

an existing survey can be exported to a new dataset, i.e., can the features learned by an unsupervised process on a given dataset be *transferred* to a new dataset with different properties? And - if not - what is the cost of updating those features (in terms of new objects to be classified from the new dataset)?

Some preliminary tests have already been performed by our team to assess the performance of DL algorithms, trained with simulated data, on real data. In a recent paper (Tuccillo et al. 2017) we show that a DL machine trained on one-component Sérsic galaxy simulations (with real HST/CANDELS F160W PSF and noise) can accurately recover parametric measurements of real HST galaxies with at least the same quality as GALFIT (Peng et al. 2002), but several orders of magnitude faster. It shows indications that DL is able to transition from simplistic simulations to real data without seriously impacting the results.

In this work we study the dependence of DL models for morphological classification of galaxies on data from different surveys. To that end, we take advantage of the DL models trained with SDSS data (presented in DS18) to test their performance when applied to DES survey, with and without training with DES images. The letter is organised as follows: In Section 2 we describe the DL models, DES images and morphological catalogue used in this work; in Section 3 we explain our methodology, in Section 4 we analyse the results and in Section 5 we summarise the conclusions of the paper.

## 2 DATA

In this paper we test the performance of DL models, trained with SDSS-DR7 data (Abazajian et al. 2009), on DES images. The morphological classification of DES galaxies comes from the DECaLS - Galaxy Zoo catalogue. In this section we describe the DL models, DES images and the morphological catalogue used throughout the paper.

### 2.1 Deep Learning models: trained with SDSS-DR7 data

In DS18 we morphologically classify ~670,000 SDSS-DR7 galaxies with automated DL algorithms. The galaxies correspond to the sample for which Meert et al. (2015, 2016) provide accurate photometric reductions. Reader can refer to DS18 for a detailed explanation on the data and methodology but, in short, we use two visual classification catalogues, Galaxy Zoo 2 (GZ2 hereafter, Willett et al. 2013) and Nair & Abraham (2010), for training CNNs with color SDSS-DR7 images. We obtain T-Types and a series of GZ2 type questions (disk/features, edge-on galaxies, bar signature, bulge prominence, roundness and mergers) for a sample of galaxies with r-band Petrosian magnitude limits  $14 \leq m_r \leq 17.77$  mag. The SDSS images are the standard cutouts downloaded from the SDSS DR7 server<sup>2</sup>, with a resolution of 0.396 ''/pixel.

<sup>1</sup> <https://www.kaggle.com/c/galaxy-zoo-the-galaxy-challenge>

<sup>2</sup> <http://casjobs.sdss.org/ImgCutoutDR7>

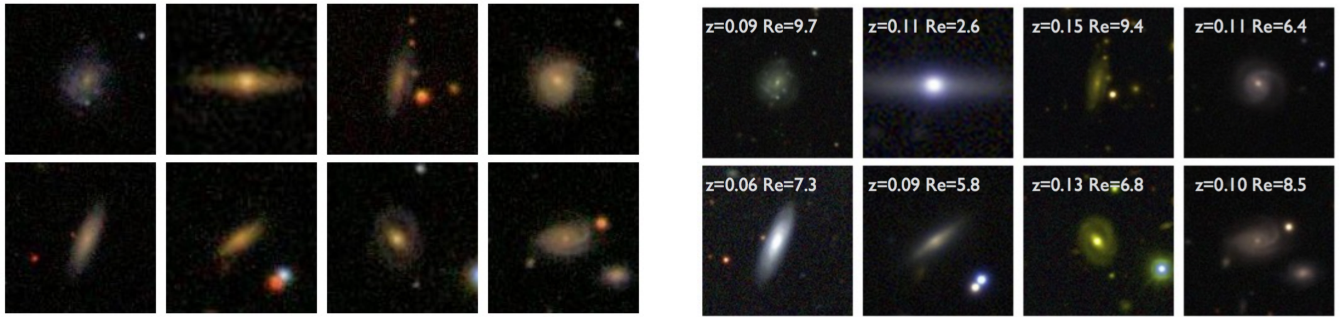


**Figure 1.** Examples of 6 galaxies observed by SDSS-DR7 (left panels) and DES survey (right panels). The cutouts are zoomed in to 1/2 of the size of the images used for training the models. They have a variable angular size of approximately  $5 \times R_{90}$ , where  $R_{90}$  is the Petrosian radius of each galaxy (shown in each cutout - in arcsec -, as well as their redshift). The galaxies are randomly selected from the common sample of the two surveys, with the only requirement of having high probability of being disk, edge-on or barred galaxies. The better quality of DES images reveals with higher detail some galaxy features, such as bulge component or spiral arms.

## 2.2 Image data: Dark Energy Survey

The images used to test how DL models can adapt to new surveys characteristics come from the Dark Energy Survey (DES; [DES Collaboration et al. 2016](#)). DES is an international, collaborative effort designed to probe the origin of the accelerating universe and the nature of dark energy by measuring almost the 14-billion-year history of cosmic expansion with high precision. The survey will map  $\sim 300$  million galaxies. This huge number demands to find automated methods for morphological classification of galaxies.

DES is a photometric survey utilizing the Dark Energy Camera (DECam; [Flaugher et al. 2015](#)) on the Blanco-4m telescope at Cerro Tololo Inter-American Observatory (CTIO) in Chile to observe  $\sim 5000$  deg $^2$  of the southern sky in five broad-band filters,  $g$ ,  $r$ ,  $i$ ,  $z$  and  $Y$  ( $\sim 400$  nm to  $\sim 1060$  nm) with a resolution of 0.263 ''/pixel. The magnitude limits and median PSF FWHM for the first year data release (Y1A1 GOLD) are 23.4, 23.2, 22.5, 21.8, 20.1 mag and 1.25, 1.07, 0.97, 0.89, 1.07 arcsec, respectively (from  $g$  to  $Y$ , see [Drlica-Wagner et al. 2017](#) for a detailed description of the survey). In this work we use standard DES cutouts from the internal Y1A1 data release.

## 2.3 Morphological catalogue: Dark Energy Camera Legacy Survey

Unfortunately, there is no morphological classification available for DES galaxies to date. Instead, we take advantage of the Galaxy Zoo Dark Energy Camera Legacy Survey (DECALS) morphological catalogue to assign a classification for DES galaxies. This is necessary for quantifying the performance of the DL models, as well as for labeling the training sample in the domain adaptation step (see section 3). The DECALS survey ([Dey et al. 2018](#)) is observed with the same camera as the DES survey and with a similar depth ( $g=24.0$ ,  $r=23.4$ ,  $z=22.5$  mag at  $5\sigma$  level), and so (average) observing conditions are very similar to the DES ones. The DECALS Galaxy Zoo catalogue (private communication) contains morphological classifications for  $\sim 32,000$  objects up to  $z \sim 0.15$ . The redshift range and most of the classification tasks are the same as for the GZ2 catalogue, which was used for training the DL models from DS18. Therefore, it is

the perfect catalogue to test the performance of the SDSS-based DL models on DES images. The main difference of DES/DECALS with respect to SDSS images is the use of a larger telescope and better seeing conditions, which allow to get deeper images ( $\sim 1.5$  mag) with significantly better data quality than SDSS. This effect can be seen in Figure 1, where we show 6 examples of galaxies as observed by SDSS and DES.

The DES sample used in this work are the 4,938 galaxies with a DECALS - Galaxy Zoo classification (obtained with a match of 1 arcsec separation). Note that, since our final aim will be to provide a morphological catalogue for DES, we use the DECALS classification catalogue as the ground truth to test (and train) our models on DES images. Given the similarities between DES and DECALS surveys, the Galaxy Zoo classifications will be identical or very similar, which allows us to perform this exercise.

## 3 METHODOLOGY

The objective of this letter is to assess if knowledge acquired by a DL algorithm from an existing survey can be exported to a new dataset with different characteristics in terms of depth, PSF and instrumental effects. This work aims to be a first *proof of concept* and not a full morphological classification catalogue. The redshift distribution of the DES galaxies used in this work is very similar to the SDSS (see 2.3), so no evolution effects are included: we are only changing the instrument and survey depth (by  $\sim 1.5$  mag). We leave for a forthcoming work a thoughtful study on the brightness and redshift effect on the models performance.

We have focused our analysis on the binary questions from the GZ2 scheme, since they are the easiest to evaluate. We note that there is one model per question. The three classification tasks that we evaluate are:

**Q1:** Galaxies with disks/features versus smooth galaxies. We consider as positive examples galaxies with disk or features (labeled as  $Y=1$  in our input matrix). **Q2:** Edge-on galaxies versus face-on galaxies. Edge-on galaxies are considered positive cases. **Q3:** Galaxies with bar signature versus galaxies with no bar presence. Barred galaxies are positive cases.

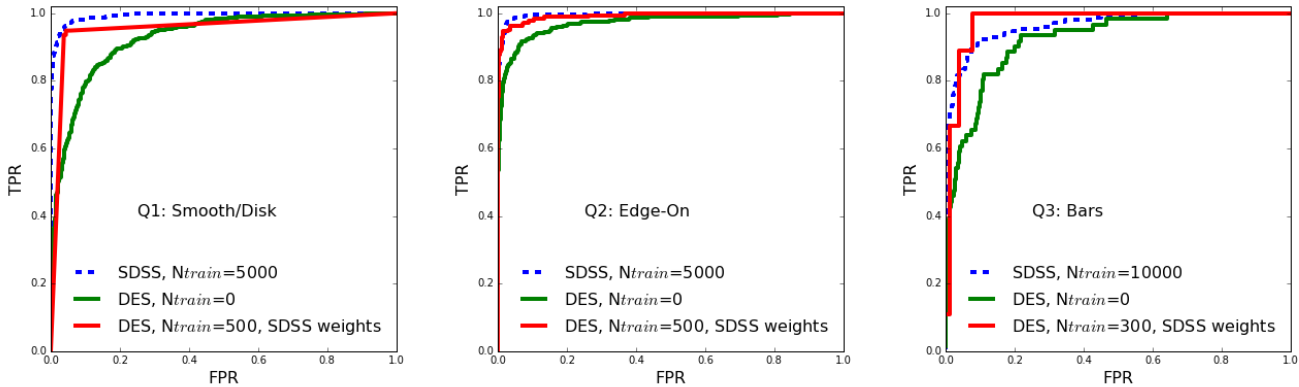


**Figure 2.** True positive rate (TPR, i.e., fraction of well classified positive cases) vs. false positive rate (FPR, i.e., fraction of wrongly classified positive cases) for different  $P_{thr}$  values for the three classification task studied in this work, as stated in the legend. We show the performance of our DL models trained with SDSS galaxies applied to SDSS images (blue dashed line), applied to DES images with no training on DES data at all (green line) and applied to DES data after a domain adaptation step using a small number of DES galaxies for re-training the models (red line). The number of galaxies used in the training for each question are shown in the legend. The results are comparable to the ones obtained for SDSS but, loading the SDSS weights to the DES-models training, helps reducing the training sample size at least one order of magnitude. The ‘apparent’ better performance of the DES model with respect to the SDSS one for Q3 is caused by the small size of the barred test sample (see Table 1).

In order to assess how much knowledge from one survey can be exported to another, we carry out two steps:

- (i) We apply the models trained on SDSS directly to DES images, without any modification at all, and study their performance on DES data. Since no training sample is used, all galaxies with a known classification can be used for testing.
- (ii) In a domain adaptation step, we train the machines with a small sample of DES galaxies (300-500) transferring the knowledge from the SDSS model. This transfer consists on loading the weights (i.e. the features) learned by the SDSS models for all the layers -both convolutional filters and dense layer- and then re-train with the DES images. The code used in this work is publicly available at <https://github.com/HelenaDominguez/DeepLearning>. We test the updated models on a sample of DES galaxies not used for training. This limits the statistics, specially in the case of Q3 (bar signature, see discussion below).

To keep the methodology as similar as possible to DS18, the input for the models are the same as in DS18, i.e. 424×424 pixel size images (from DES in this case), which are down-sampled into (69, 69, 3) RGB matrices, with each number representing the flux per pixel at each filter ( $g$ ,  $r$ ,  $i$ ). The angular size of the images is variable, approximately  $10 \times R_{90}$ , where  $R_{90}$  is the Petrosian radius of each galaxy (taken from SDSS). For test (i), the algorithm applies the weights learned by the SDSS models and returns a probability value for each task. For test (ii), we train the models in binary mode and, following DS18, we only use in the training DES galaxies with a robust classification, i.e. galaxies with a large agreement -  $a(p)$  - between Galaxy Zoo classifiers (roughly corresponding to  $P > 0.7$  in one of the two answers) and with at least 5 votes. Reader can refer to DS18 for a description of the agreement parameter,  $a(p)$ . This methodology has demonstrated to be a more efficient way to train the models, but it strongly limits the statistics of our train

and test samples. For example, only 624 out of 4938 galaxies ( $\sim 13\%$ ) have  $P_{edge-on} > 0.7$  and at least 5 votes. This number is even smaller (103,  $\sim 2\%$ ) for the barred galaxies. Since we need at least 300 galaxies for training Q3 (and the training sample should include a reasonable number of positive cases), we only have 9 barred galaxies left for testing our models (see Table 1).

## 4 RESULTS

We use a standard method for testing the performance of our models: receiver operating characteristic (ROC) curve, true positive rate (TPR), precision (P) and accuracy values (e.g., Powers & Ailab 2011, Dieleman et al. 2015, Barchi et al. 2017). For binary classifications, where only two input values are possible (positive or negative cases), the true positives (TP) are the correctly classified positive examples. One can define, in an analogous way, true negatives, false positives, and false negatives (TN, FP, FN, respectively). The true positive rate (TPR), false positive rate (FPR), precision (P) and accuracy (Acc) are expressed as:

$$\begin{aligned} TPR &= \frac{TP}{(TP + FN)}; & FPR &= \frac{FP}{(FP + TN)} \\ P &= \frac{TP}{(TP + FP)}; & Acc &= \frac{TP + TN}{Total} \end{aligned} \quad (1)$$

TPR is a completeness proxy (how many of the true examples are recovered), precision is a contamination indicator (what fraction of the output positive cases are really positive) and accuracy is the fraction of correctly classified objects among the test sample. Since the output of the model is a probability (ranging from 0 to 1), a probability threshold

Question	Survey	Ntrain	Ntest	Npos	TPR	Prec.	Acc.
Q1 Smooth/Disk	SDSS	5000	3370	674	0.93	0.91	0.97
	DES	0	2409	797	0.48	0.92	0.81
	DES	500	238	78	0.95	0.91	0.95
Q2 Edge-on	SDSS	5000	2687	396	0.98	0.80	0.96
	DES	0	2851	536	0.91	0.73	0.96
	DES	500	738	187	0.96	0.86	0.95
Q3 Bar sign	SDSS	10000	1806	169	0.76	0.79	0.96
	DES	0	1768	61	0.57	0.35	0.95
	DES	300	86	9	0.89	0.73	0.95

**Table 1.** Performance of the models according to the TPR, precision and accuracy values for the three classification tasks studied in this work. The survey column specifies the data to which the models are applied. *Ntrain* is the number of galaxies of that survey which have been used for training. When *Ntrain*=0, it means the SDSS model is directly applied to DES data. *Ntest* are the number of galaxies used for testing the models (they fulfill the requirement of having a robust morphological classification, as the training sample), of which *Npos* are the positive cases (e.g., galaxies showing disk/features for Q1). Galaxies used for training are not included in the testing sample. This explains the scarcity of barred galaxies used for testing the models with DES training.

( $P_{thr}$ ) value must be chosen to separate positive and negative cases. The ROC curve represents the TPR and FPR values for different  $P_{thr}$ . A perfect classifier would yield a point in upper left corner or coordinate (0,1) of the ROC space, (i.e., no false negatives and no false positives), while a random classifier would give a point along a diagonal line. In Figure 2 we show the ROC curve for the three classification tasks studied in this work for the SDSS model applied to SDSS data, (i) the SDSS model applied to DES data without any training on DES , and (ii) the model trained on a small DES sample, taking as a starting point the features learned by the model trained with SDSS data. In Table 1, we show the TPR, precision and accuracy values for the same cases. For simplicity, we only list the values obtained for  $P_{th}=0.5$  (the standard value for separating positive and negative cases). Both the train and test DES samples are required to have a robust classification in the morphological catalogue (see section 3). The number of galaxies used for training and testing (and the positive cases), are also given in Table 1.

Our first main result is that, when applying the SDSS-models directly to DES images, with no training at all on DES data, the accuracy values obtained are reasonable ( $> 80\%$ ), reaching 96% and 95% for Q2 and Q3. However, the accuracy can be misleading when few positive cases are included in the test sample and it is important to consider completeness and purity of the classification. These quantities are strongly dependent on the classification task. For example, for Q1 the precision value is very high (92%), but the completeness is less than 50%. On the other hand, the SDSS model recovers 91% of the DES edge-on galaxies, but the precision value for this task is 73%. For Q3, both the completeness and purity values obtained with the SDSS model are small (0.57 and 0.35, respectively). This indicates that bar identification is a very sensitive task to resolution and depth, while, on the other hand, inclination is less dependent on the survey characteristics.

The second main result is that, after a fast domain adaptation step (i.e., training the models with a small sample - less than 500 - of highly reliable DES galaxies), the models are able to adapt to the new data characteristics and quickly converge, providing results comparable to the ones

obtained for the SDSS models applied to SDSS data (see Table 1 and Figure 2). We tested the performance of the models with training samples of different sizes and we found that this is an optimal trade-off between models' results and training sample size. This means a reduction of at least one order of magnitude for the training sample with respect to training the models from scratch, and will be of major importance in order to train DL models for future Big Data surveys. The accuracy values are  $\geq 0.95$  for all the classification tasks. For both Q1 and Q2 the completeness reaches at least 95% and the purity values are 91% and 86%, respectively. The TPR and precision values for Q3 are smaller (0.89 and 0.73, respectively), but are severely affected by the test sample statistics. In fact, the model recovers 8 out of 9 barred galaxies (TP) and there are only 3 FP cases. After visual inspection, we found that the FN case is not a real barred galaxy but a bulge dominated galaxy. On the other hand, only one of the 3 FP cases have  $P_{bar} > 0.6$  according to our model, and that galaxy shows a bright central feature which could be a distorted bar or a dust lane.

## 5 CONCLUSIONS

In this paper we demonstrate that deep-nets can transfer knowledge from one survey to another and quickly adapt to new domains and data characteristics such as depth, PSF and instrumental effects.

The fact that the training sample (and therefore the a priori labeled galaxies) can be reduced by an order of magnitude, once the models are trained with a different dataset, is a major discovery in order to apply DL models to future surveys, such as EUCLID or LSST. It means that we will be able to recycle models from previous surveys (within the same redshift distribution), preventing from the huge effort of visually classifying a large sample of galaxies from that particular survey.

It is beyond the scope of this paper to test the effect of the models on more complicated aspects of galaxy surveys, such as redshift evolution. We leave for a forthcoming work this mandatory step to release a reliable morphological catalogue, which will certainly be an add-on value to the DES. Also, a major advance of extremely deep future surveys

will be the detection of features which are invisible in surveys such as SDSS or DES (e.g., tidal features and debris). Machines trained on shallower data are unlikely to produce robust results on very deep images. We plan to carry out a thorough study to this respect using cosmological hydro-dynamical simulations such as Horizon-AGN (Kaviraj et al. 2017) in a future work.

## ACKNOWLEDGEMENTS

Funding for the DES Projects has been provided by the DOE and NSF(USA), MEC/MICINN/MINECO(Spain), STFC(UK), HEFCE(UK). NCSA(UIUC), KICP(U. Chicago), CCAPP(Ohio State), MIFPA(Texas A&M), CNPQ, FAPERJ, FINEP (Brazil), DFG(Germany) and the Collaborating Institutions in the Dark Energy Survey. The Collaborating Institutions are Argonne Lab, UC Santa Cruz, University of Cambridge, CIEMAT-Madrid, University of Chicago, University College London, DES-Brazil Consortium, University of Edinburgh, ETH Zürich, Fermilab, University of Illinois, ICE (IEEC-CSIC), IFAE Barcelona, Lawrence Berkeley Lab, LMU München and the associated Excellence Cluster Universe, University of Michigan, NOAO, University of Nottingham, Ohio State University, University of Pennsylvania, University of Portsmouth, SLAC National Lab, Stanford University, University of Sussex, Texas A&M University, and the OzDES Membership Consortium. Based in part on observations at Cerro Tololo Inter-American Observatory, National Optical Astronomy Observatory, which is operated by the Association of Universities for Research in Astronomy (AURA) under a cooperative agreement with the National Science Foundation. The DES Data Management System is supported by the NSF under Grant Numbers AST-1138766 and AST-1536171. The DES participants from Spanish institutions are partially supported by MINECO under grants AYA2015-71825, ESP2015-66861, FPA2015-68048, SEV-2016-0588, SEV-2016-0597, and MDM-2015-0509, some of which include ERDF funds from the European Union. IFAE is partially funded by the CERCA program of the Generalitat de Catalunya. Research leading to these results has received funding from the European Research Council under the European Union's Seventh Framework Program (FP7/2007-2013) including ERC grant agreements 240672, 291329, and 306478. We acknowledge support from the Australian Research Council Centre of Excellence for All-sky Astrophysics (CAASTRO), through project number CE110001020, and the Brazilian Instituto Nacional de Ciéncia e Tecnologia (INCT) e-Universe (CNPq grant 465376/2014-2). This manuscript has been authored by Fermi Research Alliance, LLC under Contract No. DE-AC02-07CH11359 with the U.S. Department of Energy, Office of Science, Office of High Energy Physics. The United States Government retains and the publisher, by accepting the article for publication, acknowledges that the United States Government retains a non-exclusive, paid-up, irrevocable, world-wide license to publish or reproduce the published form of this manuscript, or allow others to do so, for United States Government purposes.

## REFERENCES

- Abazajian K. N., et al., 2009, *ApJS*, **182**, 543  
 Banerji M., et al., 2010, *MNRAS*, **406**, 342  
 Barchi P. H., da Costa F. G., Sautter R., Moura T. C., Stalder D. H., Rosa R. R., de Carvalho R. R., 2017, preprint, ([arXiv:1705.06818](https://arxiv.org/abs/1705.06818))  
 Belfiore F., et al., 2015, *MNRAS*, **449**, 867  
 Bournaud F., et al., 2014, *ApJ*, **780**, 57  
 Conselice C. J., 2003, *ApJS*, **147**, 1  
 DES Collaboration et al., 2016, *MNRAS*, **460**, 1270  
 Dey A., et al., 2018, preprint, ([arXiv:1804.08657](https://arxiv.org/abs/1804.08657))  
 Dieleman S., Willett K. W., Dambre J., 2015, *MNRAS*, **450**, 1441  
 Domínguez Sánchez H., Huertas-Company M., Bernardi M., Tuccillo D., Fischer J. L., 2018, *MNRAS*, **476**, 3661  
 Drlica-Wagner A., et al., 2017, preprint, ([arXiv:1708.01531](https://arxiv.org/abs/1708.01531))  
 Dubois Y., Peirani S., Pichon C., Devriendt J., Gavazzi R., Welker C., Volonteri M., 2016, *MNRAS*, **463**, 3948  
 Eisenstein D. J., et al., 2011, *AJ*, **142**, 72  
 Flaugher B., et al., 2015, *AJ*, **150**, 150  
 Huertas-Company M., et al., 2015, *ApJS*, **221**, 8  
 Kaviraj S., 2014, *MNRAS*, **440**, 2944  
 Kaviraj S., et al., 2017, *MNRAS*, **467**, 4739  
 LSST Science Collaboration et al., 2017, preprint, ([arXiv:1708.04058](https://arxiv.org/abs/1708.04058))  
 Lahav O., et al., 1995, *Science*, **267**, 859  
 Lahav O., Naim A., Sodré Jr. L., Storrie-Lombardi M. C., 1996, *MNRAS*, **283**, 207  
 Lintott C., et al., 2011, *MNRAS*, **410**, 166  
 Meert A., Vikram V., Bernardi M., 2015, *MNRAS*, **446**, 3943  
 Meert A., Vikram V., Bernardi M., 2016, *MNRAS*, **455**, 2440  
 Nair P. B., Abraham R. G., 2010, *ApJS*, **186**, 427  
 Newman J. A., et al., 2013, *ApJS*, **208**, 5  
 Peng C. Y., Ho L. C., Impey C. D., Rix H.-W., 2002, *AJ*, **124**, 266  
 Powers D. M. W., Ailab 2011.  
 Racca G. D., et al., 2016, in Space Telescopes and Instrumentation 2016: Optical, Infrared, and Millimeter Wave. p. 99040O ([arXiv:1610.05508](https://arxiv.org/abs/1610.05508)), doi:[10.1111/12.2230762](https://doi.org/10.1111/12.2230762)  
 Scoville N., et al., 2007, *ApJS*, **172**, 1  
 Simmons B., Lintott C., Masters K., Willett K., Kartaltepe J. S., Closson Ferguson H., Faber S. M., Galaxy Zoo Team C. T., 2016, in American Astronomical Society Meeting Abstracts. p. 342.42  
 Tuccillo D., Huertas-Company M., Decencière E., Velasco-Forero S., Domínguez Sánchez H., Dimauro P., 2017, preprint, ([arXiv:1711.03108](https://arxiv.org/abs/1711.03108))  
 Willett K. W., et al., 2013, *MNRAS*, **435**, 2835

## AFFILIATIONS

- <sup>1</sup>
- Department of Physics and Astronomy, University of Pennsylvania, Philadelphia, PA 19104, USA
- 
- <sup>2</sup>
- LERMA, Observatoire de Paris, PSL Research University, CNRS, Sorbonne Universités, UPMC Univ. Paris 06, F-75014 Paris, France
- 
- <sup>3</sup>
- University of Paris Denis Diderot, University of Paris Sorbonne Cité (PSC), 75205 Paris Cedex 13, France
- 
- <sup>4</sup>
- Centre for Astrophysics Research, University of Hertfordshire, College Lane, Hatfield, Herts AL10 9AB, UK
- 
- <sup>5</sup>
- Cerro Tololo Inter-American Observatory, National Optical Astronomy Observatory, Casilla 603, La Serena, Chile
- 
- <sup>6</sup>
- Department of Physics & Astronomy, University College London, Gower Street, London, WC1E 6BT, UK

<sup>7</sup> Department of Physics and Electronics, Rhodes University, PO Box 94, Grahamstown, 6140, South Africa

<sup>8</sup> Fermi National Accelerator Laboratory, P. O. Box 500, Batavia, IL 60510, USA

<sup>9</sup> Institute of Cosmology & Gravitation, University of Portsmouth, Portsmouth, PO1 3FX, UK

<sup>10</sup> Laboratório Interinstitucional de e-Astronomia - LIneA, Rua Gal. José Cristino 77, Rio de Janeiro, RJ - 20921-400, Brazil

<sup>11</sup> Observatório Nacional, Rua Gal. José Cristino 77, Rio de Janeiro, RJ - 20921-400, Brazil

<sup>12</sup> Department of Astronomy, University of Illinois at Urbana-Champaign, 1002 W. Green Street, Urbana, IL 61801, USA

<sup>13</sup> National Center for Supercomputing Applications, 1205 West Clark St., Urbana, IL 61801, USA

<sup>14</sup> Institut de Física d'Altes Energies (IFAE), The Barcelona Institute of Science and Technology, Campus UAB, 08193 Bellaterra (Barcelona) Spain

<sup>15</sup> Kavli Institute for Particle Astrophysics & Cosmology, P. O. Box 2450, Stanford University, Stanford, CA 94305, USA

<sup>16</sup> Centro de Investigaciones Energéticas, Medioambientales y Tecnológicas (CIEMAT), Madrid, Spain

<sup>17</sup> Department of Astronomy, University of Michigan, Ann Arbor, MI 48109, USA

<sup>18</sup> Department of Physics, University of Michigan, Ann Arbor, MI 48109, USA

<sup>19</sup> Institut d'Estudis Espacials de Catalunya (IEEC), 08193 Barcelona, Spain

<sup>20</sup> Institute of Space Sciences (ICE, CSIC), Campus UAB, Carrer de Can Magrans, s/n, 08193 Barcelona, Spain

<sup>21</sup> Kavli Institute for Cosmological Physics, University of Chicago, Chicago, IL 60637, USA

<sup>22</sup> Instituto de Física Teórica UAM/CSIC, Universidad Autónoma de Madrid, 28049 Madrid, Spain

<sup>23</sup> SLAC National Accelerator Laboratory, Menlo Park, CA 94025, USA

<sup>24</sup> Department of Physics, ETH Zurich, Wolfgang-Pauli-Strasse 16, CH-8093 Zurich, Switzerland

<sup>25</sup> Santa Cruz Institute for Particle Physics, Santa Cruz, CA 95064, USA

<sup>26</sup> Center for Cosmology and Astro-Particle Physics, The Ohio State University, Columbus, OH 43210, USA

<sup>27</sup> Department of Physics, The Ohio State University, Columbus, OH 43210, USA

<sup>28</sup> Max Planck Institute for Extraterrestrial Physics, Giessenbachstrasse, 85748 Garching, Germany

<sup>29</sup> Universitäts-Sternwarte, Fakultät für Physik, Ludwig-Maximilians Universität München, Scheinerstr. 1, 81679 München, Germany

<sup>30</sup> Harvard-Smithsonian Center for Astrophysics, Cambridge, MA 02138, USA

<sup>31</sup> Australian Astronomical Observatory, North Ryde, NSW 2113, Australia

<sup>32</sup> Department of Astrophysical Sciences, Princeton University, Peyton Hall, Princeton, NJ 08544, USA

<sup>33</sup> Institució Catalana de Recerca i Estudis Avançats, E-08010 Barcelona, Spain

<sup>34</sup> Jet Propulsion Laboratory, California Institute of Technology, 4800 Oak Grove Dr., Pasadena, CA 91109, USA

<sup>35</sup> School of Physics and Astronomy, University of Southampton, Southampton, SO17 1BJ, UK

<sup>36</sup> Brandeis University, Physics Department, 415 South Street, Waltham MA 02453

<sup>37</sup> Instituto de Física Gleb Wataghin, Universidade Estadual de Campinas, 13083-859, Campinas, SP, Brazil

<sup>38</sup> Laboratório Interinstitucional de e-Astronomia - LIneA, Rua Gal. José Cristino 77, Rio de Janeiro, RJ - 20921-400, Brazil

<sup>39</sup> Computer Science and Mathematics Division, Oak Ridge National Laboratory, Oak Ridge, TN 37831

<sup>40</sup> Institute for Astronomy, University of Edinburgh, Edinburgh EH9 3HJ, UK

This paper has been typeset from a *TeX/LaTeX* file prepared by the author.